UNIVERSITY OF OVIEDO
FACULTY OF CHEMISTRY

WAVEFUNCTION ANALYSIS. THE QTAIM AND THE MOLECULAR GRAPH.

(Physical Chemistry)

BACHELOR THESIS IN CHEMISTRY

Ana Valerio García

Oviedo, June, 2021

Contents

1 Introduction: Brief history of quantum mechanics

The development of quantum mechanics shook our image of the physical world. Understanding its origin, together with its social and political backgrounds, helps contextualising how the modern world works.

By the time the electron was discovered in 1897, its location within the atoms was completely unknown, and although electrons lie at the root of chemical behavior, the study that triggered the origin of quantum mechanics came from a completely different field, heat radiation, and from a simple plot, the spectrum of an idealised model of a perfect absorber and emitter of electromagnetic radiation, the so-called black body.

By the year 1900, many scientists were trying to come with a quantitatively accurate explanation of the spectrum of heat radiation as a function of temperature. Later that year, Berliner Max Planck disclosed a mathematical expression that fit the experimental results flawlessly. On the other hand, he could not find any classical explanation to this formula – it just worked. It was on the 14^{th} of December of 1900 when he explained that not every possible exchange of energy between the radiation field and the black body could occur, but that only some specific values were allowed. This date is considered the birthday of quantum mechanics.

These ideas led to the development of the so-called *old quantum theory*, where classical mechanics holds, but with the assumption that only some specific values of physical quantities were allowed. These quantities were said to be *quantised*. It was desired to guess a general set of quantisation rules that would operate for all circumstances. For instance, in 1905, Albert Einstein theorised that the total energy of a beam is quantised. Additionally, Arnold Sommerfeld started working on the outcomes of energy quantisation for position and speed in 1911. In that same year, Ernest Rutherford discovered the atomic nucleus. It is worth highlighting that it was in this late stage of the development of quantum mechanics when a qualitative picture of the atom was obtained. In 1913, Niels Bohr presented his quantisation ideas for the hydrogen atom.

The development of quantum mechanics was negatively affected but not completely stopped by the start of WWI in 1914. Throughout the war, in 1915, William Wilson progressed on the meaning of energy quantisation for position and speed. Sommerfeld persevered with his work in the same direction. G. N. Lewis proposed the concept of electron pairs to rationalise chemical bonds in 1916. With the truce in 1918, the work in quantum mechanics developed rapidly. This development and the investigation of issues such as the helium problem and the peculiar Zeeman effect ended in an almost total breakdown of Bohr's atomic theory in less than a year.

The development of quantum mechanics at that time took place mostly at Niels Bohr's Institute of Theoretical Physics in Copenhagen, and at the University of Göttingen in northern Germany. The most relevant participants at Göttingen were Max Born, an established professor, and Werner Heisenberg, a PhD student from Sommerfeld in Munich. Heisenberg started developing systematic tables of allowed phyisical quantities, and Born interpreted them as mathematical matrices, which was an advanced and abstract technique

back in 1925. Heisenberg polished his work and simplified the formulation. However, he worried about his scheme being inconsistent, violating the principle of conservation of energy. Several months later, Heisenberg, Born and Pascual Jordan, developed a complete and consistent quantum theory.

In 1923, Louis de Broglie vaguely associated a wave with a particle. It was Erwin Schrödinger, in 1925, who turned this idea into a theory of wave mechanics. The two versions of quantum mechanics appeared completely different, emerging a sharp debate over which of them was correct. Luckily, it was proven by Schrödinger and, independently, Carl Eckert, in 1926 that both theories were analogous to each other. It was in that same year when Schrödinger equation was postulated. Later, in 1927, Walter Heitler and Fritz London determined how to use this equation to explain how two hydrogen atoms formed a covalent bond.

With these two formulations of quantum mechanics, the quantum theory grew explosively. It easily solved the helium problem mentioned above, which collapsed the old quantum theory. This theory answered questions regarding the structure of stars, the nature of superconductors, and the properties of magnets. A very important actor, P.A.M. Dirac, extended the theory to relativistic and field-theoretic scenarios in 1926. Additionally, in 1931, Linus Pauling developed quantum mechanical concepts to explain chemical bonding by using both Lewis and Heitler-London ideas. Furthermore, John C. Slater introduced the Slater determinant in 1929 for confirming the anti-symmetry of a many-electron wave function,[1] although the wave function only appeared in a determinant format in Heisenberg's and Dirac's articles in 1932. In this same year, Robert Mulliken introduced the concept of orbital, who primarily worked on the molecular orbital (MO) theory (1933) – a method describing the electronic structure of molecules using quantum mechanics – with Friedrich Hund.[2]

2 Methods

2.1 Aims

The main aim of this thesis is to calculate the wave function for a set of different molecules and extract its chemical information by making use of mathematical tools such as *quantum chemical topology* (QCT) and the quantum theory of atoms in molecules (QTAIM). With this chemical information, it will be proven that the molecular graph, which is a fuzzy concept derived from experience that tends to use accepted knowledge and tables of interatomic distances, can be built from a molecule's wave function through the use of the critical points of the electron density scalar field, which can be extracted computationally.

Different groups of molecules, such as aliphatic hydrocarbons, organic cyclic compounds, polar inorganic compounds and hypervalent halogen compounds, are subject to analysis. Calculations are performed with *Avogadro*, *Orca* and *AIMall* computer programs, employing the *variational Hartree-Fock* method with a basis set composed of Gaussian-Type orbital functions (GTO), which will allow a mathematical description of the molecular orbitals of the compounds to be analysed.

2.2 The basis of the QM formalism as applied to Chemistry

In this section, different methods employed in quantum mechanics for the calculation and understanding of wave functions are discussed. Such methods include the explanation and physical meaning of familiar terms, such as operators, Slater determinants, the Born-Oppenheimer approximation, the variational principle, Pauli's principle, and how they are applied and support the QM methods of interest in this project.

Once the quantum mechanics formalism was developed thanks to the work of Born, Heisenberg, Schrödinger, *etc*, all the information from the wave function and its evolution is translated thanks to the application of an object called *operator*. The equation of the evolution of the wave function is called *Schrödinger's equation*.

2.2.1 Operators and their properties

Operators play a key role in quantum mechanics. They *operate* on a function to produce a new function. Additionally, every physical magnitude has an operator associated to it. Being the time-dependent Schrödinger equation in one dimension for a single particle of mass m and wave function ψ:

$$i\hbar\frac{\partial\psi(x,t)}{\partial t} = -\frac{\hbar^2}{2m}\frac{\partial^2\psi(x,t)}{\partial x^2}, \tag{1}$$

where i is the imaginary unit, $\hbar$ is the reduced Planck's constant, x is position and t is time.

The square of the wave function, ψ^2, is interpreted, after the Copenhaguen interpretation, as the probability of finding the particle at a given point in space. Being this a

probability, its integration must equal 1, since the particle must be located somewhere in the physical space.

The Hamiltonian operator, $\hat{H}$, which corresponds to the total energy of a system including kinetic and potential energy, is expressed for a single-particle system as follows:

$$\hat{H} = \frac{\hat{p}^2}{2m} + \hat{V}, \tag{2}$$

where $\hat{p}$ is the momentum operator and $\hat{V}$ is the potential energy operator.

The right-hand side of (1) is $-(\hbar^2/2m)\nabla^2$, whereas in momentum space, it equals $\hat{p}^2/2m$. This involves:

$$\hat{p}^2 = -\hbar^2\nabla^2. \tag{3}$$

Now, the operator $\hat{V}$ is defined as:

$$\hat{V}f(\mathbf{r}) = V(\mathbf{r})f(\mathbf{r}), \tag{4}$$

where $\mathbf{r}$ is the position.

In (4), $\hat{V}$ is acting on $f(\mathbf{r})$ – this operator picks up the value of the potential at the $\mathbf{r}$ position, and then multiplies by $f(\mathbf{r})$. By making use of (3), a complete description of the Hamiltonian operator is obtained:[3]

$$\hat{H}\psi(\mathbf{r},t) = \left[\frac{\hat{p}^2}{2m} + \hat{V}\right]\psi(\mathbf{r},t) = \left[-\frac{\hbar^2\nabla^2}{2m} + V(\mathbf{r})\right]\psi(\mathbf{r},t). \tag{5}$$

Regarding the *properties* of operators in quantum mechanics, it is assumed that all operators are lineal and **Hermitian**, which play a key role in this field.

In order to understand the concept of Hermiticity, the expectation value of an operator needs to be introduced. The expectation value of an operator $\hat{A}$, equal to the scalar product $\left(\psi, \hat{A}\psi\right)$, is independent of momentum or coordinate space being used for the wave function. While the operator $\hat{A}$ is time-independent, its expectation value, $\langle\hat{A}\rangle$, is not:

$$\langle\hat{A}\rangle = \int d\mathbf{r}\psi^*(\mathbf{r},t)\hat{A}\psi(\mathbf{r},t) = \int d\mathbf{p}\Phi^*(\mathbf{p},t)\hat{A}\Phi(\mathbf{p},t), \tag{6}$$

where Φ is the wave function in momentum space.

An operator is Hermitian when $\left(\hat{A}\psi, \psi\right) = \left(\psi, \hat{A}\psi\right)$. In Dirac's notation, $\langle\ \psi|\hat{A}|\psi\rangle$. They are associated with every measurable dynamic physical observable. Moreover, there is a complete set of eigenfunctions $\psi_a(\mathbf{r})$ related to the Hermitian operator $\hat{A}$, such that:

$$\hat{A}\psi_a(\mathbf{r}) = a\psi_a(\mathbf{r}). \tag{7}$$

Hence, if a property of a particle is measured, one of the possible eigenfunctions of the operator associated to that property is found. Additionally, when the eigenfunctions and eigenvalues of the energy operator are found, the wave function of the system can be determined.

It is only when two operators commute that both their properties can be measured simultaneously. Considering that operators do not necessarily commute in quantum mechanics, the *commutator* $\hat{C}$ of two operators $\hat{A}$ and $\hat{B}$ is defined as:

$$\hat{C} = \left[\hat{A}, \hat{B}\right] = \hat{A}\hat{B} - \hat{B}\hat{A} = -\left[\hat{B}, \hat{A}\right]. \tag{8}$$

If the Hamiltonian of a system is time-independent, then we can separate variables to obtain particular solutions which are stationary. To that end, we write the wave function as a product of a time-dependent phase factor and a spatial term. Calling E the separation constant,

$$\psi\left(\mathbf{r}, t\right) = \varphi(\mathbf{r})\Phi(t), \tag{9}$$

$$\hat{H}\psi = i\hbar\frac{\partial}{\partial t}\psi, \tag{10}$$

$$\Phi = e^{\frac{-iEt}{\hbar}}, \tag{11}$$

$$\hat{H}\varphi_E(\mathbf{r}) = E\varphi_E\mathbf{r}. \tag{12}$$

where equation (12) is the time independent Schrödinger equation, and E becomes identified with the energy of the state described by ψ.

Equation (12) represents an eigenvalue equation, where E is the eigenvalue and $\varphi_E(\mathbf{r})$ is the corresponding eigenfunction. When solutions to equations of this kind are always available, the operators are Hermitian (*vide infra* **Section 3.4.1**). Additionally, the eigenfunctions of a Hermitian operator can be automatically orthogonal or can be selected to be orthogonal.

To summarise, the importance of operators is clear when stating that, by finding the eigenfunctions and eigenvalues of the Hamiltonian operator, all properties of quantum systems can be derived.[4]

2.2.2 Particle statistics

When working with non-relativistic Hamiltonian operators, the concept of electron spin as an *ad hoc* quantum effect must be established.

In quantum mechanics, elemental particles can be grouped in particles with spin $\frac{1}{2}$ (*fermions*) and particles with integer spin 1, 2, 3, *etc* (*bosons*). Electrons have a spin $\frac{1}{2}$, i.e., they are fermions. In the presence of a magnetic field, the two states $m_s = \pm\frac{1}{2}$ are revealed. These states correlate with the orientation towards the field. The analogous spin functions are orthonormal, and are referred to α and β for orientations along and

opposite to the field, respectively.

$$\begin{aligned} \langle\alpha|\alpha\rangle &= \langle\beta|\beta\rangle = 1. \\ \langle\alpha|\beta\rangle &= \langle\beta|\alpha\rangle = 0. \end{aligned} \tag{13}$$

Exact solutions to the Schrödinger equation are only available for simple systems such as the hydrogen atom, and other systems containing only one electron. For more complex systems, approximate solutions must be generated by making use of the of the *variational principle*, which states that any approximate wave function has an energy greater than the exact energy, or equal only if the wave function is exact. This principle also determines the best set of single-electron wave functions, or *orbitals*. In addition, an orbital in a molecule is called a *molecular orbital*.

The energy of an approximate wave function can be expressed as:

$$E_e = \frac{\langle\psi|\hat{H}_e|\psi\rangle}{\langle\psi|\psi\rangle}, \tag{14}$$

where E_e is the electronic contribution to the energy, and H_e is the electronic Hamiltonian.

Wave functions must be normalised so that $\langle\psi|\psi\rangle = 1$. Thus, (14) can be simplified to $E_e = \langle\psi|\hat{H}_e|\psi\rangle$. Additionally, the total electronic wave function must be **antisymmetric** with respect to the interchange of any two electron coordinates. This condition is in agreement with the *Pauli Exclusion principle*, which claims that two electrons cannot occupy the same quantum state. On the other hand, in the case of bosons, there is no limitation as to more than two particles occupying the same quantum space.

If the wave function is not antisymmetric by itself, this requirement can be accomplished by constructing trial wave functions from single *Slater determinants*. These determinants have single-electron wave functions (or orbitals), ϕ, occupying their columns and electron coordinates filling their rows. In addition, the Slater determinant must be normalised. For that, it is essential that ϕ_i and ϕ_j are orthonormal:

$$\langle\phi_i|\phi_j\rangle = \delta_{ij}. \tag{15}$$

For a general case of N electrons and N spinorbitals, the Slater determinant is given as:[4]

$$\Phi_{SD} = \frac{1}{\sqrt{N!}} \begin{vmatrix} \phi_1(1) & \phi_2(1) & \dots & \phi_N(1) \\ \phi_1(2) & \phi_2(2) & \dots & \phi_N(2) \\ \vdots & \vdots & \ddots & \vdots \\ \phi_1(N) & \phi_2(N) & \dots & \phi_N(N) \end{vmatrix}; \langle\phi_i|\phi_j\rangle = \delta_{ij}, \tag{16}$$

where $\delta_{ij} = 1$ when $i = j$.

A Slater determinant is the simplest solution to the Schrödinger equation, implying

that electron correlation is ignored, i.e., that electron- electron repulsion are only included as an average effect.

2.2.3 The Born-Oppenheimer approximation

When the Schrödinger equation is being solved for a molecule, two types of particles are present: electrons and *nuclei*. The wave function will then depend on electron coordinates, $\mathbf{r}_i$, and nuclei coordinates, $\mathbf{R}_i$.

The **Born-Oppenheimer approximation** (BO) is the assumption that electronic and nuclear wave functions can be treated separately. The total, non-relativistic, Hamiltonian operator can be expressed by means of the kinetic and potential energies of the nuclei and electrons.

$$\hat{H}_{total} = \hat{T}_n + \hat{T}_e + \hat{V}_{ne} + \hat{V}_{ee} + \hat{V}_{nn}, \tag{17}$$

where $\hat{T}_n$ is the operator for the kinetic energy of the nuclei, $\hat{T}_e$ is the electronic kinetic energy operator, $\hat{V}_{ne}$ is the operator for the attractive nucleus-electron potential, $\hat{V}_{ee}$ is the repulsive electron-electron potential operator, and $\hat{V}_{nn}$ is the repulsive nucleus-nucleus potential operator.

This approximation contemplates electrons to move in the ambit of a defined potential, whereas the nuclei remain fixed. This assumption arises from the difference in mass between electrons and nuclei. The kinetic energy of the nuclei equals $\frac{\hat{p}_N^2}{2M_N}$ – which is inversely proportional to the mass. Hence, the kinetic energy of the nuclei can be considered to be negligible when compared to the electronic kinetic energy. Under this situation, the Hamiltonian of the system can be expressed solely as the electronic Hamiltonian.

$$\hat{H}_{elec} = \hat{T}_e + \hat{V}_{ne} + \hat{V}_{ee} \tag{18}$$

$$= -\frac{1}{2}\sum_{i=1}^{N}\nabla_i^2 - \sum_{i=1}^{N}\sum_{A=1}^{M}\frac{Z_A}{|\mathbf{r}_i - \mathbf{R}_A|} + \sum_{i>j}^{N}\frac{1}{|\mathbf{r}_i - \mathbf{r}_j|}. \tag{19}$$

After applying the BO approximation, it is not wrong to express the time-independent Schrödinger equation solely in electronic terms and the repulsion between the nuclei:

$$E_{total} = E_{elec} + \sum_{A>B}\frac{Z_A Z_B}{|\mathbf{R}_A - \mathbf{R}_B|}, \tag{20}$$

where E_{elec} is one of the eigenvalues of the electronic Hamiltonian.

Nevertheless, it could not be possible to locate nuclei in space if the Born-Oppenheimer approximation is not applied. In addition, without this approximation, the concept of molecular geometry would not be plausible anymore. This would also not be reasonable when more than one solution to the Schrödinger equation are very close in energy. The geometry of the molecule varies, and the wave function tends to degeneracy.[4]

2.2.4 The SCF approximation, Hartree-Fock methods

In the case of a wave function being obtained as a Slater determinant, the best possible orbitals need to be chosen. These are obtained from the **Self-Consistent Field theory** or **Hartree-Fock method**. Numerical Hartree-Fock methods are employed for highly symmetric system, such as atoms and diatomic molecules, while algebraic ones, based on expanding orbitals in a fixed basis, are used for larger systems.

The desired orbitals, i.e., those leading to the smallest energy, can be obtained by minimisation by using Lagrange multipliers that force the mutual orthonormality of the different functions.

$$L = E - \sum_{ij}^{N} \lambda_{ij} \left(\langle \phi_i | \phi_j \rangle - \delta_{ij} \right), \tag{21}$$

where L is the Lagrangian and λ is the Lagrange multiplier.

It can be seen that the term in parenthesis in (21) cancels out in the final solution, given the condition specified by (15). Hence, the minimum in energy is obtained. In the same way, the final set of Hartree-Fock equations is written as:

$$\hat{F}_i \phi_i = \sum_{j}^{N_{elec}} \lambda_{ij} \phi_j, \tag{22}$$

being $\hat{F}$ an operator called the Fockian operator.

Finally, the orbital energy, ϵ_i, is expressed as follows:

$$\epsilon_i = \langle \phi_i | \hat{F}_i | \phi_j \rangle = h_i + \sum_{j}^{N_{elec}} \left(J_{ij} - K_{ij} \right), \tag{23}$$

where h is the monoelectronic Hamiltonian. J accounts for Coulomb integrals and K for exchange integrals.

Nonetheless, the total energy of the system is not the sum of all molecular orbital energies. The Fock operator includes terms accounting to all other electrons ($\hat{J}$ and $\hat{K}$ operators). Simply summing over molecular energies would count the interelectron repulsion twice, which is incorrect and must be rectified.[4]

2.2.5 Electron correlation and post-HF methods

The Hartree-Fock method produces solutions to the Schrödinger equation where the electron-electron interaction is approximated by an average interaction. Hence, some of the total energy is not considered due to this approximation.

The difference in energy amidst the HF and the lowest energy in the specific basis set is termed *Electron Correlation* (EC) energy.[5]

$$E_{corr} = E_{exact(non-relativistic)} - E_{HF}, \tag{24}$$

where E_{exact} is the exact, non-relativistic energy, and E_{HF} is the energy obtained through Hartree-Fock methods.

Whilst the size of the molecule increases, the number of electron pairs belonging to the different spatial molecular orbitals enlarge faster than the referred ones to the same molecular orbital.

Opposite spin correlations can also be known as *Coulomb correlation*. Additionally, for correlations for same spin electrons, an alternative term is the *Fermi correlation*, being the former contribution greater than the latter.

There can also be *dynamic* and *static* electron correlation. The former is related with instant correlation between electrons, i.e., electrons situated in the same spatial orbital. Nevertheless, the static part relates with electrons evading each other on a permanent manner, i.e., electrons situated in different spatial orbitals.[4]

2.2.6 The algebraic approximation

In most cases, each orbital ϕ is expanded as a linear combination of a set of fixed functions, called basis functions, χ, or atomic orbitals in a relaxed language. However, these are typically not solutions to the atomic Hartree-Fock problem. The algebraic approximation finds these linear coefficients and transforms the Hartree-Fock integro-differential equations into matrix equations. Each orbital is thus written as

$$\phi_i = \sum_{\alpha}^{M_{basis}} c_{\alpha i}\chi_\alpha, \tag{25}$$

where c are molecular orbital coefficients.

Basis sets expansions are virtually employed to express unknown molecular orbitals in terms of a set of known functions. Two steps for choosing the basis functions are needed:

1. The behaviour of such functions must match with the physics of the issue. This guarantees convergence as more basis functions are added rapidly.

2. The chosen functions should make it easy to calculate all the required integrals. This condition is a practical one.

Even though the first measure recommends using exponential functions located on the nuclei, this is a difficult task computationally speaking. On the other hand, Gaussian functions are computationally much easier to deal with. Nevertheless, these functions provide poorer descriptions of electronic structures, but the computational effort being decreased is worth the loss of accuracy. For a deeper description of basis sets, *vide infra* **Section 2.2.7**.

The Hartree-Fock equations can be written as an alternative to (22):

$$\mathbf{F}_i \sum_{\alpha}^{M_{basis}} c_{\alpha i}\chi_\alpha = \epsilon_i \sum_{\alpha}^{M_{basis}} c_{\alpha i}\chi_\alpha. \tag{26}$$

When multiplying this expression from the left by a given basis function and integrating, the *Roothaan-Hall* equations are obtained,[6] which determine the eigenvalues and eigenvectors of the Fock Matrix. These are the HF equations in the atomic orbital basis. All the M_{basis} equations can be summarised in a matrix fashion:

$$\mathbf{FC} = \mathbf{SCE}, \tag{27}$$

$$F_{\alpha\beta} = \langle\chi_\alpha|\,\mathbf{F}\,|\chi_\beta\rangle\,, \tag{28}$$

$$S_{\alpha\beta} = \langle\chi_\alpha|\chi_\beta\rangle\,, \tag{29}$$

where $\mathbf{S}$ is a matrix containing the overlap integrals between basis functions, $\mathbf{E}$ is a diagonal matrix that contains the different orbital energies and $\mathbf{C}$ is the matrix of coefficients used in equation (26).

Each $F_{\alpha\beta}$ element holds two portions from the Fock operator: integrals dealing with one-electron operators and a sum over occupied MOs of coefficients multiplied with two-electron integrals involving electron repulsion.

$$F_{\alpha\beta} = h_{\alpha\beta} + \sum_{\gamma\delta} G_{\alpha\beta\gamma\delta} D_{\gamma\delta}, \tag{30}$$

$$\mathbf{F} = \mathbf{h} + \mathbf{G}\cdot\mathbf{D}, \tag{31}$$

$$\mathbf{D} = \mathbf{C}^\dagger\mathbf{C} = \begin{pmatrix} \mathbf{D}^{AA} & \mathbf{D}^{AB} & \mathbf{D}^{AC} & \dots \\ \mathbf{D}^{AB} & \mathbf{D}^{BB} & \mathbf{D}^{BC} & \dots \\ \mathbf{D}^{AC} & \mathbf{D}^{BC} & \mathbf{D}^{CC} & \dots \\ \vdots & \vdots & \vdots & \ddots \end{pmatrix}, \tag{32}$$

where h is the one-electron (core) matrix, $\mathbf{D}$ is the so-called density matrix and $\mathbf{G}\cdot\mathbf{D}$ represents the contraction of the so-called density matrix with the four-dimensional $\mathbf{G}$ tensor.

Additionally, the total energy in terms of integrals over basis functions can be expressed as:

$$E = \sum_{\alpha\beta}^{M_{basis}} D_{\alpha\beta} h_{\alpha\beta} + \frac{1}{2} \sum_{\alpha\beta\gamma\delta}^{M_{basis}} \left(D_{\alpha\beta} D_{\gamma\delta} - D_{\alpha\delta} D_{\gamma\beta}\right) \langle\chi_\alpha\chi_\gamma|\,\mathbf{g}\,|\chi_\beta\chi_\delta\rangle + V_{nn}. \tag{33}$$

To determine the unknown MO coefficients $c_{\alpha i}$ in (29), the Fock matrix must be diagonalised. Since the Fock matrix is only known if all MO coefficients are known, the approach begins by guessing some of the coefficients, forming said matrix and diagonalising it. Iteratively, the new set of coefficients are employed for calculating a new Fock matrix, until all the coefficients equal the ones obtained from diagonalisation. This set of coefficients determines the SCF solution.[4]

2.2.7 Basis sets

The basis set approximation is employed to reveal the unknown molecular orbitals of a system. To determine the molecular orbital coefficients, the **Fock matrix** must be analysed.

Since the Fock matrix is only established when all molecular orbital coefficients are known, a new set of coefficients are used for calculating a new Fock matrix. One-electron integrals, also known as core integrals, are required for building this matrix. These integrals are one-dimensional. Additionally, these are *ab initio* HF methods. An iterative process is carried out until the set of molecular orbitals equals those resulting from diagonalisation.

Following the variational principle, the greater the number of basis functions, the better the accuracy of the molecular orbitals. However, an increase in the number of basis functions also means more time-consuming calculations. Given that the computational effort of *ab initio* methods scales at least M_{basis}^4, it is essential to find a compromise between using a small basis set without jeopardising the accuracy[7]. In order to achieve a relatively fast convergence, the choose of basis set must be in accordance with the physics of the problem. Another requirement is for the chosen functions to make it easy to calculate the required integrals.

Nevertheless, in the limit of a complete basis set, results match the ones obtained by numerical Hartree-Fock methods. This limit is never achieved in practical calculations, and could not be the exact solution to the Schrödinger equation.[4]

The two types of basis functions frequently used in electronic structure calculations are *Slater Type Orbitals* (STO) and *Gaussian Type Orbitals* (GTO). None of these functions have any radial nodes.

Slater type orbitals[8] are of the form:

$$\chi_{\zeta,n,l,m}(R,\theta,\varphi) = NY_{l,n}(\theta,\varphi)\, r^{n-1} e^{-\zeta r}, \tag{34}$$

where N is the normalisation constant and $Y_{l,m}$ are the spherical harmonic functions.

Moreover, Gaussian type orbitals can be written in terms of polar or Cartesian coordinates:[9]

$$\chi_{\zeta,n,l,m}(r,\theta,\varphi) = NY_{l,m}(\theta,\varphi)\, r^{2n-2-l} e^{-\zeta r^2}, \tag{35}$$

$$\chi_{\zeta,l_x,l_y,l_z}(x,y,z) = N x^{l_x} y^{l_y} z^{l_z} e^{-\zeta r^2}, \tag{36}$$

where the sum of l_x, l_y and l_z determines the type of orbital.

More GTOs are needed for fulfilling a given accuracy compared with STOs. Nevertheless, three times as many GTOs as STOs are indispensable for getting to a given level of accuracy.

On the other hand, increasing the number of GTO basis functions is more computationally efficient as a consequence of their ease of which the required integrals can be

calculated. GTOs are almost universally used in electronic structure calculations,[4] and will be the ones chosen in the development of this thesis.

The next enhancement is doubling, tripling and even quadrupling all basis functions, as well as including *polarisation* and *diffuse* functions. Polarisation functions are functions of larger angular momentum value than that of the electron configuration of the atom that is being described, and are used to correct for the lower symmetry of atoms in molecular environments with respect to the atomic ones. Diffuse functions are slowly decaying functions used when dealing with long-range interactions or excited states. Adding these types of functions improves the accuracy of the results – yet, more computational effort is required.

3 Wavefunction analysis

While theoretical chemistry provides energies, it does not provide chemical information attached to it straightforwardly. How this information is extracted is usually called *wave function analysis*.

3.1 From ψ to chemistry: population analysis – Mulliken and Löwdin problems

The concept of population analysis involves isolating atoms within molecules from a previously calculated wave function. The simplest wave function analysis method is called the *Mulliken population analysis*. This method uses the $\mathbf{D} \cdot \mathbf{S}$ matrix – which requires an explicit calculation of the $\mathbf{S}$ matrix (29) – for allotting the electrons into atomic contributions.[10] An additional frequently used method is the *Lödwin* partitioning, consisting in the use of the $\mathbf{S}^{\frac{1}{2}} \cdot \mathbf{D} \cdot \mathbf{S}^{\frac{1}{2}}$ matrix for wave function analysis.[11] In both cases we come with the so-called gross populations, which are found as diagonal elements of a matrix and provide information about the number of electrons residing in an atom, and the overlap populations, coming from non-diagonal elements, which inform about bond orders. There are many common problems with these type of population analysis based on partitioning the wave function in terms of basis functions:

1. Diagonal elements could be larger than two. This would involve more than two electrons per orbital, violating the Pauli principle.

2. Off-diagonal elements can become negative. This implies a negative number of electrons between two basis functions, which clearly is physically impossible.

3. There is no unbiased motive for dividing the off-diagonal contributions evenly between the two orbitals. The most electronegative atom should take most of the shared electrons.

4. Basis functions centered on atom A may have small exponents, describing electrons far from this atom. Additionally, the electron density − probability of finding an electron − is counted as only be owned by A.

5. Dipole, quadrupole, *etc*, moments are generally not conserved: an arrange of population atomic charges does not reproduce the original multipole components.

The Mulliken method suffers from all mentioned problems, whereas the Löwdin approach solves problems 1, 2 and 3.

The primary issue relies in basis functions describing electron density near the nucleus instead of the one they are centred on. Atomic charges calculated from Mulliken or Löwdin methodologies will not converge to a constant value as the size of basis set is enlarged. This ususally involves adding more diffuse basis functions, heading to unpredictable changes in atomic charges.[4]

In order to solve these problems, other methods not depending on orbitals have been proposed. To understand these methods, the electron density function will be defined in the next section.

3.2 Electron density and its Laplacian

The electron density is defined as the number of electrons per unit volume element. It is designated by $\rho(\mathbf{r})$ and its formula in terms of the wave function ψ is:

$$\rho(\mathbf{r}) = N \int \cdots \int |\psi(\mathbf{x}_1, \mathbf{x}_2, \ldots, \mathbf{x}_N)|^2 ds_1 d\mathbf{x}_2 \ldots d\mathbf{x}_N, \tag{37}$$

where s_1 is the spin coordinate for electron 1, and x_i are the spatial and spin coordinates of the electrons.

This is a positive simple function of three variables (x, y, z) that integrates to the total number of electrons N:

$$\int \rho(\mathbf{r}) d\mathbf{r} = N. \tag{38}$$

It is clear that if a region for each atom could be defined, then the number of electrons for a particular atom could be obtained by integrating ρ in its region, as equation (38) states. This is what the topological method provides: a way of distributing the space in regions associated to atoms.

For atoms in their ground state, it is known that the electron density decays uniformly away from the nucleus.[12] In the case of molecules, densities are close to superimposed atomic densities, although a more rigorous analysis shows slight accumulations of density present in bonding sections.[13]

Since the wave function is expressed in terms of a single Slater determinant for Hartree-Fock (and *density functional*) theories, the electron density can be reduced to

$$\rho(\mathbf{r}) = \sum_{k=1}^{N} n_k |\phi_k(\mathbf{r})|^2, \tag{39}$$

where n_k is the occupation number of each orbital, equal to 1 or 2.

Another concept of great interest for this thesis is the Laplacian of the electron density, $\nabla^2\rho$. It measures the local curvature of a function in all its dimensions, three for ρ. The Laplacian contains a lot of valuable chemical information, it helps revealing further information about ρ, and it supports the VSEPR model,[14] which is used in chemistry to predict the structure of molecular compounds from the number of electron pairs surrounding their central atoms.

The Laplacian is the trace of the second derivatives matrix of ρ, the Hessian, and thus it is also equal to the sum of its eigenvalues, as it will be described in the following section. It can be shown that when the sign of the Laplacian is negative, the value of $\rho(\mathbf{r})$

is greater than the average of its values over an infinitesimal sphere with centre $\mathbf{r}$. The contrary is true if the Laplacian is positive at a given point.

Local accumulations are decoupled from the value of the density itself. There is a possibility where the electron density has a small value while being locally accumulated and, on the other hand, the opposite situation can be found near the nucleus: the electron density can be very high at some points, but locally depleted. The measure of $\nabla^2\rho$ describes how strong the effect of concentration or depletion is.[15] The sign of the Laplacian of the electron density can describe whether there is a local accumulation or leakage in the charge. Having $\nabla^2\rho < 0$ means a local accumulation of charge with respect to its vicinity. On the other hand, $\nabla^2\rho > 0$ means that the charge is depleting in regard to its surroundings.[20]

3.3 The topological approach

Provided that density functional theory proves that the electron density contains all the information necessary to reconstruct the wave function of the system, and thus its energy, a number of authors envisioned that the study of this scalar field would also be important to formalise the concepts of the theory of chemical bonding. This is possible after a partition of the physical space $\mathbb{R}^3$ is performed.[16]

In this section, quantum chemical topology (or QCT), which consists of a series of methods dealing the topology of a scalar field to extract chemical information from systems, will be discussed.

3.3.1 Topology of a scalar field: critical points, gradient fields and basins

Being the electron density a physical quantity with a definite value at each point in space, it is also a scalar field defined over the three-dimensional space. The topological approach of this scalar field is explained with regard to number and type of critical points. These are points where the gradient of a function vanishes. There can be maxima, minima, and saddle points, and each type of critical point can be determined by the sign of its second derivative or *curvature*, as it will be seen later.

Critical points of a scalar f are characterised for being points where the gradient vector, ∇f, equals 0. The characterisation of CPs is done by employing a 3×3 matrix involving second derivatives, called the *Hessian* matrix. Three eigenvalues are obtained when the matrix is diagonalised, and said eigenvalues can take different structures. A more detailed view of the Hessian matrix is developed in **Section 3.4.1**.

The topology induced by the density scalar is obtained by studying the associated gradient vector field – whose properties are characterised by associating both a direction and a magnitude – of the electron density: $\nabla\rho(\mathbf{r})$, which vanishes at critical points. If starting from a point we follow the gradient vector, a gradient trajectory of steepest slope develops until a maximum in the electron density is reached or a $\nabla\rho = 0$ point is found. Due to the behavior of the electron density, maxima coincide (almost always) with nuclei. The set of points whose gradient lines end up at a given nuclei form its attraction basin.

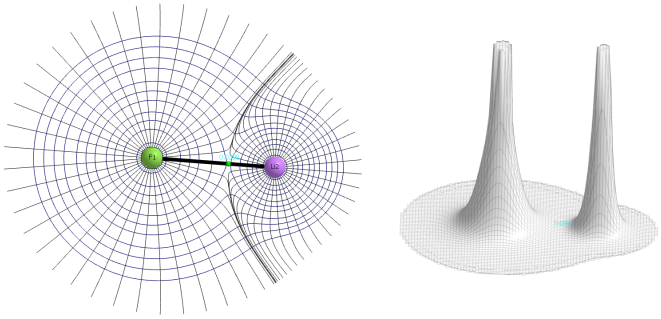

Figure 1: Left: Graphical representation of the isolines of ρ and the position of the bond critical point (BCP) for lithium fluoride. Fluorine atom at the left and lithium atom at the right. The separatrix and the gradient field lines, showing the steepest path following the isolines, are shown for each atom. Right: Relief map for the electron density of LiF in 3D and its BCP position. Fluorine atom at the left and lithium atom at the right. Minimum electron density $\rho = 0.0001$. Images generated with *AIMall*[17] by analysing the *Orca*[18] output of a HF optimization using a def2-TZVP basis set.

Attraction basins are separated by the so-called separatrices. All non-nuclear critical points of the field are located on these surfaces. An example of the topology of ρ can be found in figure 3.3.1 for the LiF molecule.

There exist four possible types of critical points in the electron density, each of them related to a specific chemical object. Besides the nuclear points we find bond, ring, and cage critical points.

For a random selection of coordinate axes, nine second derivatives of the type $\frac{\partial^2 \rho}{\partial x \partial y}$ exist in the resolution of the curvatures of the electron density at a point in space. This 3×3 array is denoted as the *Hessian matrix* of ρ. Since this is a real, symmetric matrix, it can be diagonalised – this is equivalent to finding a rotation of the coordinate axes such that all the off-diagonal elements become zero. The three eigenvalues are the curvatures of the density along the direction of the new principal axes.

$$H = \begin{pmatrix} \frac{\partial^2 \rho}{\partial x^2} & \frac{\partial^2 \rho}{\partial x \partial y} & \frac{\partial^2 \rho}{\partial x \partial y} \\ \frac{\partial^2 \rho}{\partial y \partial x} & \frac{\partial^2 \rho}{\partial y^2} & \frac{\partial^2 \rho}{\partial y \partial z} \\ \frac{\partial^2 \rho}{\partial z \partial x} & \frac{\partial^2 \rho}{\partial z \partial y} & \frac{\partial^2 \rho}{\partial z^2} \end{pmatrix}. \tag{40}$$

As it was mentioned in the previous section, the sum of the diagonal elements of the Hessian matrix corresponds to the Laplacian and it is invariant to a rotation of the coordinate system.

$$\nabla^2 \rho = \nabla \cdot \nabla \rho = \frac{\partial^2 \rho}{\partial x^2} + \frac{\partial^2 \rho}{\partial y^2} + \frac{\partial^2 \rho}{\partial z^2}. \tag{41}$$

Critical points are classified firstly through the *rank*, ω, which equals to the number of non-zero eigenvalues or non-zero curvatures of the electron density at the CP. Additionally, the *signature*, σ, is the algebraic sum of the signs of eigenvalues. Hence, the critical point

is labelled as (ω, σ) [19] (*vide infra* **Section 3.4.1**).

If we start a gradient line along the principal curvatures at a critical point we can have two behaviors: convergence (attraction) toward the CP if the eigenvalue is negative or divergence (repulsion) if it is positive. If there are three negative eigenvalues (e.g., at a nucleus) then we find a 3D region of gradient lines converging toward it. This is the attraction basin. If there are two negative eigenvalues there is an attracting surface and a repulsive line, an attracting line and a repulsive surface when there is one, and a 3D repulsion basin when the three eigenvalues are positive. Thus the flow of $\nabla\rho$ around a CP allows to classify it according to the dimensionality of its **basin of attraction** or **basin of repulsion**.

Neglecting surfaces, lines, or points with respect to bulk 3D regions, the full space can thus be decomposed into a finite number of subsets if we use the attraction basins of the maxima or the repulsion basins of the minima. Since maxima coincide (almost always) with nuclei, the first partition is an atomic one. The surfaces separating these atomic basins are zero flux surfaces[20]:

$$\int_S \nabla\rho(\mathbf{r}) \cdot n(\mathbf{r}) ds = 0. \tag{42}$$

3.4 The QTAIM

The QTAIM, or *quantum theory of atoms in molecules*, emerges from applying the QCT to the electron density – a scalar field – due to the fact that the topology divides the three dimensional space into atoms, and atoms show maxima in electron density.

This theory provides expected values for each subsystem, which will be called *atomic observable*. Any molecular observable can be built from atomic observables.[20]

3.4.1 Properties at CPs

As it was mentioned earlier, the QTAIM provides abundant profitable chemical information. To extract this information, the properties at critical points need to be known.

In this thesis, critical points with $\omega = 3$ are studied. There are four possible signature values for this constraint:[19]

- (3, -3) – all curvatures are negative and ρ is a local maximum at $\mathbf{r}_c$. This type of critical points is nuclear attractor, or NACP.
- (3, -1) – two curvatures are negative and ρ is a maximum at $\mathbf{r}_c$ in the place defined by their corresponding axes. ρ is a minimum at $\mathbf{r}_c$ along the third axis, which is perpendicular to this plane. This corresponds to a BCP, or bond critical point.
- (3, +1) – two curvatures are positive and ρ is a minimum at $\mathbf{r}_c$ in the plane defined by their corresponding axes. ρ is a maximum at $\mathbf{r}_c$ along the third axis which is perpendicular to this plane. This describes a RCP, or ring critical point.

- (3, +3) – all curvatures are positive and ρ is a local minimum at $\mathbf{r}_c$. This type of critical point is a cage one, or CCP.

Bond critical points appear between two atoms that are understood to be linked. Accumulation of electron density between nuclei translates into an increase in inter-nuclear density, hence, stronger bonding.

In the QTAIM, operators must be Hermitian so real solutions of the Schrödinger equation can be obtained.[20] The hermiticity condition in real space looks as:

$$\int (\hat{H}\psi)^* \psi d\mathbf{r} = \int \psi^* (\hat{H}\psi) d\mathbf{r}, \tag{43}$$

which holds for the full space but not necessarily for a spatial domain Ω.

One of the operators affected by this constraint is the kinetic energy operator, $\hat{T}$:

$$\hat{T} = \frac{p^2}{2m} = \frac{-\hbar^2}{2m}\nabla^2. \tag{44}$$

After performing several mathematical transformations, $\hat{T}$ can be expressed as:

$$\frac{\hbar^2}{4m}\int_\Omega (\nabla^{2\prime} + \nabla^2)\rho(\mathbf{r};\mathbf{r}')|_{\mathbf{r}\to\mathbf{r}'} d\mathbf{r} = \frac{\hbar^2}{2m}\int_\Omega \nabla'\nabla\rho(\mathbf{r};\mathbf{r}')|_{\mathbf{r}\to\mathbf{r}'} d\mathbf{r} - \frac{\hbar^2}{4m}\oint_S \nabla\rho\cdot d\mathbf{S}. \tag{45}$$

Two feasible kinetic energy densities are introduced: K, which accounts for the Laplacian contribution, and G, a **positive definite density** corresponding to gradient contributions:

$$K = -\frac{\hbar^2}{4m}(\nabla^{2\prime} + \nabla^2)\rho(\mathbf{r};\mathbf{r}'). \tag{46}$$

$$G = \frac{\hbar^2}{2m}\nabla'\nabla\rho(\mathbf{r};\mathbf{r}'). \tag{47}$$

And also an operator directly correlated with the Laplacian of the electron density, L:

$$L = -\frac{\hbar^2}{4m}\nabla^2\rho. \tag{48}$$

Hence, (45) can be expressed as:

$$\int_\Omega K(\mathbf{r})d\mathbf{r} = \int_\Omega G(\mathbf{r})d\mathbf{r} - \int_\Omega \nabla^2\rho\mathbf{r}d\mathbf{r}, \tag{49}$$

$$K_\Omega = G_\Omega + L_\Omega. \tag{50}$$

The $-\int_\Omega \nabla^2\rho(\mathbf{r})d\mathbf{r}$ term, which corresponds to L, equals zero if the region is one of the regions of the QTAIM. In this case, the kinetic energy of an atomic region is well defined.[20]

The density along a bond path is minimum at the critical point. Here, the Hessian matrix has a positive eigenvalue along the direction of curvature being tangent to the

bond path, and two negative eigenvalues along the two directions generating the tangent plane to the interatomic surface. Let us call this curvatures λ_1, λ_2 and λ_3. The ellipticity ϵ of a BCP can be defined as

$$\epsilon = \frac{\lambda_1}{\lambda_2} - 1. \tag{51}$$

This magnitude is correlated with the π character of a chemical bond. Additionally, the π character of a bond is not an observable magnitude. However, it is linked to a type of orbital description. Nevertheless, ϵ measures the anisotropy in an electron density distribution, having no direct information about the orbital contribution of said anisotropy.[20]

Another useful magnitude related to the π character of a bond is the *delocalisation index*:

$$DI(A,B) = 2\int_A\int_B \rho_{xc}\left(\mathbf{r}_1,\mathbf{r}_2\right) d\mathbf{r}_1 d\mathbf{r}_2, \tag{52}$$

where A and B are two quantum atoms and $\rho_{xc}(\mathbf{r}_1,\mathbf{r}_2)$ is the exchange-correlation density.

The exchange-correlation density is formally equal to $\rho_1(\mathbf{r}_1)\rho_1(\mathbf{r}_2) - \rho_2(\mathbf{r}_1,\mathbf{r}_2)$, and it is sometimes defined with opposite sign. By solving equation (52) averaging the exchange-correlation density over a pair of basins, a measure of the number of electron pairs that are being shared between quantum atoms A and B is obtained, i.e. this magnitude is a direct representation of the bond order.[21]

4 Results and discussion

4.1 The problem to be solved

The main problem to be solved in this work consists in solving the Schrödinger equation, from which the wave function is obtained, therefore the electron density distribution, for a set of different molecules. From this density distribution chemical information will be extracted by making use of QCT. A proper understanding of the bonding behavior and topology of the electron density leads to a good interpretation of the energy and equilibrium geometry of a molecule. We will show that the topology of the electron density allows to build automatically the molecular graph of a molecule.

We understand as **molecular graph** a mathematical undirected graph where a vertex is associated to each of the nuclei of a system and an edge is placed between each pair of vertices to which a chemical bond is assigned.

4.2 Systems studied, computational conditions, basis sets, validation

Different sets of molecules have been studied by making use of different computational programs, such as *Avogadro*,[22] *Orca*,[18] and *AIMall*.[17] The different groups of molecules to be studied are the following:

- **Aliphatic hydrocarbons**: methane, ethane, ethene and ethyne.
- **Polar inorganic compounds**: hydrogen oxide, ammonia, phosphine, lithium fluoride and hydrochloric acid.
- **Cyclic organic molecules**: ethylene oxide, cyclopropane, cyclobutane, cyclobutadiene, cyclohexane (chair conformation) and benzene.
- **Hypervalent halogens**: chlorine trifluoride, chlorine pentafluoride, bromine trifluoride oxide.

An adequate basis set was chosen for performing the calculations. As it was previously discussed in **Section 2.2.7**, the greater the number of Gaussian basis functions, the more accurate the results, but also the greater the computational effort. A compromise between accurate results and less time-consuming operations must be found for the development of all the calculations. To simplify as much as possible, the Hartree-Fock approximation has been chosen.

Input files are created with *Avogadro*, where a scheme of the molecular geometry is drawn and its energy is optimised in order to get the most stable geometry using a very cheap force field. For the basis set validation method, an ethane molecule is drawn and different *input* files are created including the different basis sets to be analysed. *Input* files for basis set validation test can be found in appendix 1.

For a given molecule, results are considered valid when its total energy does not differ more than $4kJ/mol$ ($1.5936 \cdot 10^{-3} E_h/mol$) from its reference value provided in the text

by Jensen.[4] Considering this, a basis set validation method for ethane (total energy $-79.2587 E_h^{[23]}$) can be found in table 1.

Basis set	# Gaussian functions	Total energy (E_h)	Total run time (s)
def2-SVP	90	-79.17288286	10
def2-TZVP	140	-79.25679678	11
def2-TZVPP	188	-79.25865137	25
def2-QZVPP	352	-79.26271189	312
ma-def2-SVP	98	-79.17339469	5
ma-def2-TZVP	148	-79.25681211	13
ma-def2-TZVPP	196	-79.25868101	29
ma-def2-QZVPP	360	-79.26271371	376

Table 1: Basis set validation test for ethane. Calculations performed with *Orca* through a numerical HF method. All data in a.u.

Given the compromise between level of accuracy and shortest analysis time, the most suitable basis set is the *def2-TZVP*, a *triple zeta valence polarised* basis set. It could be logical to consider picking a basis set where the accuracy is even better but computational time is slightly greater. On the other hand, ethane is a rather simple molecule, and the more complex molecules employed in this thesis would make the computational effort scale considerably (at least M_{basis}^4). Thus, the selected basis set functions will provide accurate and fast results.

It is worth mentioning that this validation method will be employed for all types of molecules analysed in this work. It is not the aim of this work to find a particular basis set for each type of molecule and calculations developed here, and that is why this validation test will be extrapolated.

Once the adequate basis set is chosen, the required calculations for the rest of the molecules are performed with *Orca* in the same manner. Prior generation of *input* files including the desired basis set are created and optimised with *Avogadro.*

4.3 A case in detail

A particular molecule is described in detail in this section. The selected molecule to be described is benzene, belonging to the family of aromatic cyclic compounds in organic chemistry. This molecule has been chosen due to its variety of critical points and bond behavior – benzene possess nuclear attractor critical points, bond critical points with different bond orders, and a ring critical point given that it is a cyclic compound. Additionally, benzene belongs to the D_{6h} point group:[24] its high symmetry allows a great simplification of its data since all hydrogen and carbon atoms are equivalent among each other.

The molecular graph of benzene in figure 3 shows C-C and C-H bonds as they are expected with their usual bond distances.

The Mulliken atomic charges are +0.1254 for carbon and -0.1254 for hydrogen. Given that there are six carbon atoms and six hydrogen atoms, the net charge of the molecule equals 0.

NO LB	X	Y	Z
0 C	-7.848656	4.905748	-0.000000
1 C	-7.763316	2.263306	0.000000
2 C	-5.432226	1.015992	-0.000000
3 C	-3.186494	2.411120	-0.000000
4 C	-3.271834	5.053543	-0.000000
5 C	-5.602906	6.300857	-0.000000
6 C	-9.652041	5.870699	-0.000000
7 H	-5.668933	8.345125	-0.000000
8 H	-9.500674	1.184008	0.000000
9 H	-5.366218	-1.028257	0.000000
10 H	-1.383091	1.446170	-0.000000
11 H	-1.534458	6.132861	-0.000000

Table 2: Cartesian coordinates of benzene in a.u. generated with *Orca* using the HF method and a def2-TZVP basis set. It can be observed it is a planar molecule given that all coordinates in the Z axis are 0.

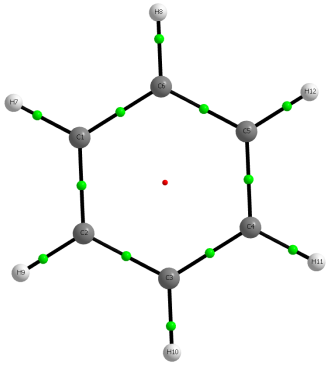

Table 3: Molecular graph of benzene visualised with *AIMall*. BCPs are shown in green. Image generated with *AIMall* by analysing *Orca* through the HF method using a def2-TZVP basis set.

Considering the structure of benzene, twelve NACPs i.e., one for each nucleus, twelve BCPs and one RCP are determined, satisfying the Poincare-Hopf Relationship, which states that $Num_{NACP} + Num_{NNACP} - Num_{BCP} + Num_{RCP} - Num_{CCP} = 1$. The values of the electron density, Laplacian and ellipticity are almost identical between C-C BCPs, suggesting that all these six bonds are identical. The same happens with the C-H bonds: they show almost the same values for the before mentioned parameters, suggesting all C-H bonds are equivalent. A summary of these values can be found in table 4.

Type of CP	Atom(s)	ρ	$\nabla^2\rho$	ϵ	K	DI(A,B)
NACP	C	122.1	NA	NA	NA	NA
NACP	H	0.4355	NA	NA	NA	NA
RCP	C ring	0.0221	0.1473	NA	-0.0047	NA
BCP	C-C	0.3259	-1.0678	0.2162	0.3644	1.3921
BCP	C-H	0.2939	-1.1201	0.01540	0.3149	0.9692

Table 4: Critical points for Benzene, where the type of CP, electron density and its Laplacian, ellipticity, kinetic energy and delocalisation indexes DI(A,B) are included. All data in a.u. Results generated with *AIMall* performing a QTAIM study with the HF method and a def2-TZVP basis set using *Orca*.

Regarding ρ in the carbon and hydrogen NACPs, their high values are expected, given that these CPs are located in the nucleus of each atom. The difference in value accounts also for the difference in size between carbon and hydrogen. A greater value is expected for a bigger atom, given that the electron cloud surrounding its nucleus will be bigger as well.

In relation to the RCP of benzene concerning all carbon atoms forming the aromatic ring, its low value of the electron density shows that the probability of finding an electron in that region is rather low. The positive value of the Laplacian shows that there is actually a local charge loss with respect to its surroundings.

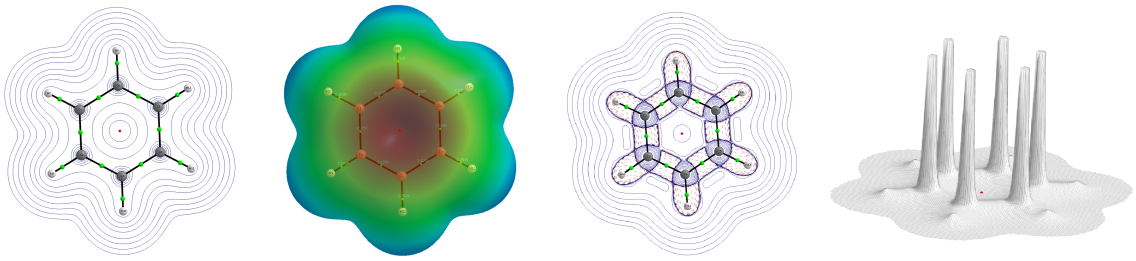

Figure 2: From left to right: contour map of the electron density in 2D, contour map of the electron density in 3D showing the total electrostatic potential, Laplacian and relief map of the electron density for benzene. All figures in the plane containing the twelve nuclei. Images generated with *AIMall* by analysing *Orca* with the HF method and a def2-TZVP basis set.

Concerning the BCPs of benzene, the values for ρ in the carbon-carbon bonds are larger than the values for the carbon-hydrogen bond. These values suggest that both types of bonding are covalent – given that a covalent bond is characterised by the sharing of electron pairs between atoms. Anyhow, the higher value of the C-C bond has the physical meaning of a higher probability of finding electrons in that region of space, suggesting that the C-C bond is stronger than the C-H bond.

The ellipticity of a BCP is directly related with the π character of a bond. This value in the C-C BCP is an indicator of its partial double bond.[20] This idea can also be supported by looking at the delocalisation index, DI(A,B). The value of 1.3921 in the C-C BCP means that this bond is in a state between single and double, which justifies the π cloud within the aromatic ring in this molecule. On the other hand, the C-H bond gives a value very close to 1 – this bond is a single covalent one.

4.4 Aliphatic hydrocarbons

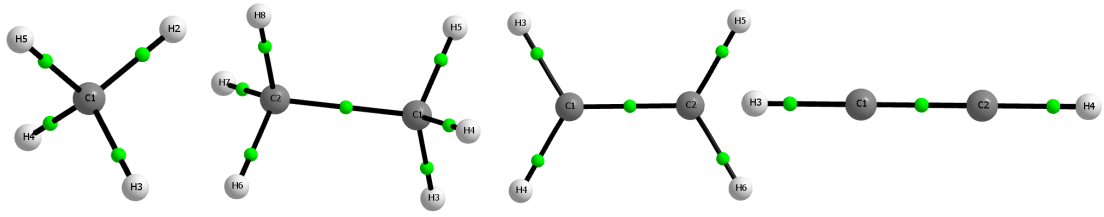

Figure 3: Molecular graphs of methane, ethane, ethene and ethyne. BCP shown in green. Images generated with *AIMall* by analysing *Orca* through the HF method using a def2-TZVP basis set.

In this section, compounds shown in figure 3 are described. The parameters to be discussed are found in table 5.

Concerning atomic charges, all molecules are neutral. Regarding ρ at the nuclei, all values are quite similar for H ($\sim$ 0.4) and for C ($\sim$ 122). The negative value of the Laplacian at the BCPs can be interpreted as an accumulation of negative charge located

Molecule	Type of CP	q	ρ	$\nabla^2\rho$	ϵ	K	DI(A,B)
Methane, T_d	NACP, C	0.0347	121.9	NA	NA	NA	NA
	NACP, H	-0.0087	0.4196	NA	NA	NA	NA
	BCP, C-H	NA	0.2713	-0.9585	0.0000	0.2761	0.9818
Ethane, D_{3d} (Staggered)	NACP, C	0.0882	121.9	NA	NA	NA	NA
	NACP, H	-0.0294	0.4256	NA	NA	NA	NA
	BCP, C-C	NA	0.2606	-0.7546	0.0000	0.2429	1.0104
	BCP, C-H	NA	0.2733	-0.9704	0.0029	0.2796	0.9644
Ethene, D_{2h}	NACP, C	-0.0355	122.1	NA	NA	NA	NA
	NACP, H	0.0177	0.4312	NA	NA	NA	NA
	BCP, C-C	NA	0.3662	-1.2500	0.3907	0.4538	1.8982
	BCP, C-H	NA	0.2903	-1.0969	0.0119	0.3087	0.9775
Ethyne, $D_{\infty h}$	NACP, C	-0.1803	122.3	NA	NA	NA	NA
	NACP, H	0.1803	0.4146	NA	NA	NA	NA
	BCP, C-C	NA	0.4186	-1.2378	0.0000	0.6167	2.8710
	BCP, C-H	NA	0.3019	-1.2210	0.0000	0.3358	0.9549

Table 5: Topological indexes for the aliphatic hydrocarbons studied. The point group of each molecule,[24] type of CP and atoms involved, electron density and its Laplacian, ellipticity, kinetic energy and delocalisation indexes are displayed in this table. All data in a.u. Results generated through a QTAIM study with *AIMall* by analysing them with *Orca* through the HF method using a def2-TZVP basis set.

at the bond critical point, i.e., covalent character. Additionally, the greater the value of ρ in BCPs the stronger the bond at which that BCP is contained: C-C bonds are stronger than C-H bonds.

The most interesting feature to discuss in this section is the delocalisation index DI(A,B). As it was mentioned before, this index is directly correlated with the π character of a bond. Hence, it is also correlated with its bond order, BO. Being methane a molecule with one carbon atom linked to four hydrogen atoms, there is no other possibility for the bonds to be single since it is physically unachievable for hydrogen ($Z = 1$) to form multiple bonds. This is also supported by its value of bond ellipticity (0.00), which shows no π character. In the case of ethane, ethene and ethyne, which are linear molecules containing two carbon atoms, the values of DI(A,B) provide chemical information about their bond multiplicity. Being these values 1.0104 for ethane, 1.8982 for ethene and 2.8710 for ethyne, their C-C bonds are single, double and triple, respectively. This statement is in accordance with the usual representation of these molecules, and can also be supported with their values of bond ellipticities. For ethane, the value of 0.00 means a total absence of π character, whereas the value of 0.3907 in ethene shows it. On the other hand, ethyne has a value of 0.00 for the ellipticity even though it is well known that this bond has a strong π character. This can be explained by the symmetry of this molecule ($D_{\infty h}$) and its linearity. Nonetheless, having a value of $DI(A, B) > 1$ confirms π character in the molecule. On a side note, the value of the kinetic energy K proportionally increases with the number of electrons. This is a general trend and it will be applied on the following sections in the same manner.

4.5 Cyclic organic compounds

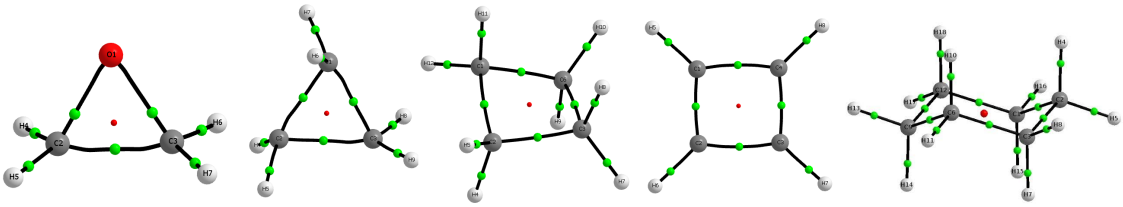

Figure 4: Molecular graphs of ethylene oxide, cyclopropane, cyclobutane, cyclobutadiene and cyclohexane (chair conformation). BCPs represented in green. Images generated with *AIMall* by analysing *Orca* with the HF method using a def2-TZVP basis set.

By looking at the molecular graphs (figure 4) generated by performing a QTAIM study, it cannot be denied that molecular graphs can be constructed by a QCT analysis, finding their respective CPs (table 6) that lead us to locate nuclei in space and their corresponding bonds. As it can be seen in figure 2 in section 4.3, further properties of the CPs can be visualised, such as the local charge accumulation and depletion, represented by the Laplacian of the electron density.

For these compounds, as well as for the previous aliphatic compounds, the negative value of the Laplacian at the BCPs shows covalent character. In the case of cyclobutadiene, the smallest π conjugated system, it can be seen that one type of C-C bond is single and the other has double character. This can be concluded by looking at the values of DI(A,B). In contrast to benzene, where all C-C bonds are equivalent with $DI(A,B) = 1.3921$, cyclobutadiene has 4n π electrons, making this system *antiaromatic*, which makes this molecule unstable. This involves having the π electrons located within bonds possessing double character rather than forming an electron cloud.

It is worth pointing out the strain of these cyclic compounds. As it can be seen in figure 4, the bonds are not entirely linear. This has been successfully related to the concept of strain. Cyclobutane can be the highlight regarding this property: this molecule adopts a puckered conformation (figure 5), in a similar way cyclohexane adopts the chair conformation in its most stable form. Altogether, puckering and non-linear BCP lines make the C-C-C angles approach the tetrahedral ones.

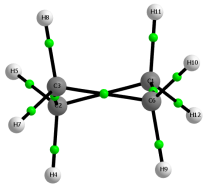

Figure 5: Cyclobutane molecular graph showing its puckered confirmation. BCPs are shown in green. Image visualised with AIMall by analysing *Orca* with the HF method using a def2-TZVP basis set.

It is interesting to talk about the electron density at the RCPs. In the case of ethylene

Molecule	Type of CP	q	ρ	$\nabla^2\rho$	ϵ	K	DI(A,B)
Ethylene oxide, C_{2v}	NACP, C	0.5043	122.0	NA	NA	A	NA
	NACP, H	0.0464	0.4223	NA	NA	NA	NA
	NACP, O	-1.1939	301.8	NA	NA	NA	NA
	RCP	NA	0.2237	0.1561	NA	0.1640	NA
	BCP, C-C	NA	0.2561	-0.6340	0.4473	0.2483	0.8974
	BCP, C-H	NA	0.2822	-1.0489	0.0305	0.2897	0.9259
	BCP, C-O	NA	0.2634	-0.2932	0.6851	0.4026	0.8942
Cyclopropane, D_{3h}	NACP, C	-0.0619	121.9	NA	NA	NA	NA
	NACP, H	0.0310	0.4160	NA	NA	NA	NA
	RCP	NA	0.2034	0.0178	NA	0.1345	NA
	BCP, C-C	NA	0.2397	-0.5125	0.6258	0.2204	0.9785
	BCP, C-H	NA	0.2731	-0.9689	0.0380	0.2771	0.9530
Cyclobutane, D_{2d}	NACP, C	0.06	122.0	NA	NA	NA	NA
	NACP, $H_{equat.}$	-0.03	0.4263	NA	NA	NA	NA
	NACP, H_{axial}	-0.04	0.4258	NA	NA	NA	NA
	RCP	NA	0.0951	0.3891	NA	0.0165	NA
	BCP, C-C	NA	0.2586	-0.7291	0.0128	0.2400	0.9709
	BCP, C-$H_{equat.}$	NA	0.2751	-0.9914	0.0040	0.2824	0.9602
	BCP, C-H_{axial}	NA	0.2712	-0.9544	0.0043	0.2758	0.9484
Cyclobutadiene, D_{2h}	NACP, C	-0.0491	122.2	NA	NA	NA	NA
	NACP, H	0.0481	0.4241	NA	NA	NA	NA
	RCP	NA	0.1164	0.5891	NA	0.0285	NA
	BCP, C-C_{double}	NA	0.3676	-1.2199	0.4480	0.4570	1.8404
	BCP, C-C_{single}	NA	0.2875	-0.9115	0.0035	0.2950	1.0129
	BCP, C-H	NA	0.2900	-1.1048	0.0274	0.3089	0.9704
Cyclohexane, D_{3d} (chair)	NACP, C	0.0906	121.9	NA	NA	NA	NA
	NACP, H_{axial}	-0.046898	0.4293	NA	NA	NA	NA
	NACP, $H_{equat.}$	-0.043957	0.4293	NA	NA	NA	NA
	RCP	NA	0.0205	0.1069	NA	-0.0025	NA
	BCP, C-C	NA	0.2563	-0.7276	0.0001	0.2342	0.9744
	BCP, C-H_{axial}	NA	0.2732	-0.9686	0.0026	0.2800	0.9419
	BCP, C-$H_{equat.}$	NA	0.2744	-0.9774	0.0011	0.2818	0.9507

Table 6: Topological indexes for the cyclic organic compounds studied. The point group of each molecule,[24] type of CP and atoms involved, electron density and its Laplacian, ellipticity, kinetic energy and delocalisation indexes are displayed in this table. All data in a.u. Results generated through a QTAIM study with *AIMall* by analysing them with *Orca* with the HF method using a def2-TZVP basis set.

Molecule	Type of CP	q	ρ	$\nabla^2\rho$	ϵ	K	DI(A,B)
H_2O, C_{2v}	NAPC, H	0.5994	0.3878	NA	NA	NA	NA
	NACP, O	-1.1988	301.4	NA	NA	NA	NA
	BCP, O-H	NA	0.3371	-2.2641	0.0225	0.6257	0.6501
NH_3, C_{3v}	NACP, H	-1.1097	0.4052	NA	NA	NA	NA
	NACP, N	0.3699	198.2	NA	NA	NA	NA
	BCP, N-H	NA	0.3175	-1.4744	0.0413	0.4185	0.8722
PH_3, C3v	NACP, H	-0.5810	0.3716	NA	NA	NA	NA
	NACP, P	1.7698	2104.0	NA	NA	NA	NA
	BCP, P-H	NA	0.1570	-0.0571	0.1188	0.1478	0.8153
HCl	NACP, H	0.3285	0.3105	NA	NA	NA	NA
	NACP, Cl	-0.3285	3101.0	NA	NA	NA	NA
	BCP, H-Cl	NA	0.2047	-0.5336	0.0000	0.1675	0.9417
LiF	NACP, F	-0.9479	434.9	NA	NA	NA	NA
	NACP, Li	0.9479	13.42	NA	NA	NA	NA
	BCP, Li-F	NA	0.0390	0.3207	0.0000	-0.0113	0.1353

Table 7: Topological indexes for the polar inorganic compounds studied. The point group of each molecule,[24] type of CP and atoms involved, electron density and its Laplacian, ellipticity, kinetic energy and delocalisation index are displayed in this table. All data in a.u. Results generated through a QTAIM study with *AIMall* by analysing them with *Orca* with the HF method using a def2-TZVP basis set.

oxide and cyclopropane, the value of ρ is very similar to the values at the BCPs. On the other hand, the value of $\nabla^2\rho$ is positive, which shows a local depletion in the charge in that region. Nevertheless, the values of ρ decrease in the tendency: cyclobutane, cyclobutadiene and cyclohexane – electron density in the RCP decreases when the C-C-C angle increases. Such increase in angle can be manifested in their molecular graphs presented in figure 4. Note how, for cyclobutane and cyclohexane, not all the hydrogens – and C-H bonds – are equivalent. This can be explained by the fact that some of the hydrogens are in equatorial positions whereas others are in axial positions. This statement is in accordance with how these molecular graphs are constructed regarding their bond distances and angles, meaning that graphs generated by computational methods, in this case QCT, are valid and reliable. Additionally, the value of the Laplacian decreases as well, still keeping the positive sign, which means more local charge depletion in the RCP region.

4.6 Polar inorganic compounds

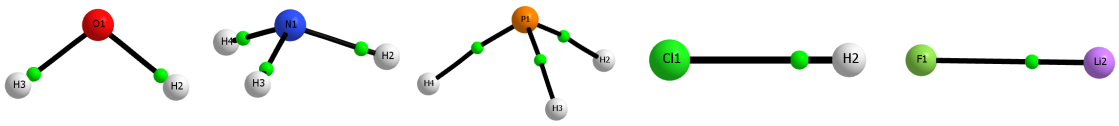

Figure 6: Molecular graphs of hydrogen oxide, ammonia, phosphine, hydrochloric acid and lithium fluoride. BCPs are shown in green. Images generated with *AIMall* by analysing them with *Orca* with the HF method using a def2-TZVP basis set.

As one can observe in the atomic charges of these compounds (table 7), they are neutral

molecules. Nevertheless, this group of molecules shows different properties compared to previous ones: these molecules are highly polarised with a higher electron density near the most electronegative atom due to their lone pair electrons. This can be explained with the delocalisation indexes: their low values at the BCPs are due to the polarity of these molecules. The very low value of DI for LiF (0.1353) reveals why this is the bond with the highest dipole moment among all these molecules, as it is expected due to the difference in electron density between lithium and fluorine.

In consideration of bonding, while all compounds showing negative value of $\nabla^2\rho$ at their BCPs contain covalent bonds, an exception for lithium chloride where its Laplacian is positive happens: the Li-F bond has ionic character, which is not surprising due to the electron transfer from metal atom (Li) to non-metal atom (F). Moreover, the covalent compounds showing non-zero delocalisation indexes suggest electron delocalisation withing bonds.

On a side note, it is compelling to compare ammonia and phosphine molecules: even though the point group between these two molecules is identical, it is not hard to see that if we add the BCPs to the molecular graphs they differ clearly – while nitrogen is one of the most electronegative atoms in the periodic table, placing the BCP considerably near the hydrogen atoms, phosphorous is not: the BCP is somewhat in the middle position of the bond path. P-H bonds are also stretched, and hold significantly higher values of ϵ compared to N-H bonds.

4.7 Hypervalent halogen compounds

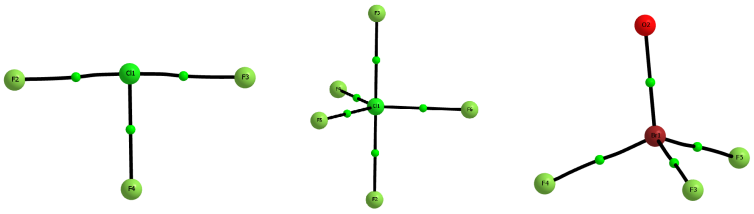

Figure 7: Molecular graphs of chlorine trifluoride, chlorine pentafluoride and bromine trifluoride oxide. BCPs shown in green. Images generated with *AIMall* by analysing them with *Orca* with the HF method using a def2-TZVP basis set.

This section is devoted to the study of hypervalent hylogens (figure 7). As one may find in table 8, the central atoms in these molecules are positively charged; yet, the net charge of the molecules is zero, i.e., they are neutral. The main focus in this section is to determine whether the central atom has an expanded octet or not. This question can be answered and easily proved by examining the values obtained by QCT.

The values of $\nabla^2\rho$ in BCPs for chlorine trifluoride are negative, meaning that, at first glance, these bonds would have some covalent character. On the other hand, if the values of the Laplacian for the equatorial F are compared with the axial ones, the latter are much smaller than the former – the Cl-F_{axial} bond is more ionic and highly polarised. This fact is also supported with the charge of axial fluorides and their delocalisation index, which

Molecule	Type of CP	q	ρ	$\nabla^2\rho$	ϵ	K	DI(A,B)
ClF_3, C_{2v}	NACP, Cl	1.522715	3103	NA	NA	NA	NA
	NACP, F_{axial}	-0.585713	435.5	NA	NA	NA	NA
	NACP, $F_{equat.}$	-0.350687	435.9	NA	NA	NA	NA
	BCP, Cl-F_{axial}	NA	0.1914	-0.0992	0.2269	0.1589	0.8696
	BCP, Cl-$F_{equat.}$	NA	0.2075	-0.2375	0.2293	0.1655	0.9990
ClF_5, C_{4v}	NACP, Cl	2.4330	3109.0	NA	NA	NA	NA
	NACP, F_{axial}	-0.5211	435.63	NA	NA	NA	NA
	NACP, $F_{equat.}$	-0.4639	435.63	NA	NA	NA	NA
	BCP, Cl-F_{axial}	NA	0.2074	0.1393	0.0808	0.1376	0.7987
	BCP, Cl-$F_{equat.}$	NA	0.2095	0.0435	0.0001	0.1491	0.8674
BrF_3O, C3v	NACP, Br	2.7083	28800	NA	NA	NA	NA
	NACP, F	-0.6332	435.6	NA	NA	NA	NA
	NACP, O	-0.8090	302.7	NA	NA	NA	NA
	BCP, Br-F	NA	0.1530	0.1918	0.0096	0.0928	0.7521
	BCP, Br-O	NA	0.2595	-0.0864	0.0000	0.2547	1.6108

Table 8: Topological indexes for the hypervalent halogen compounds studied. The point group of each molecule,[24] type of CP and atoms involved, electron density and its Laplacian, ellipticity, kinetic energy and delocalisation index are displayed in this table. All data in a.u. Results generated through a QTAIM study with *AIMall* by analysing them with *Orca* through the HF method using a def2-TZVP basis set.

show a more ionic behavior. A graphical representation of this phenomena (figure 8) shows the bond character of these molecules.

In the case of ClF_5 and BrF_3O, the halogen-halogen BCPs show a small but positive value of the Laplacian, which can be translated in local charge depletion in that region, i.e., ionic character bonds. Nonetheless, the Br-O bond in bromine trifluoride oxide shows a covalent character due to the small but negative value of the Laplacian. Additionally, even though the bond ellipticity equals 0, suggesting there is no π character within this bond is incorrect – the non-zero value of DI(A,B) says otherwise: there is electronic delocalisation in this region.

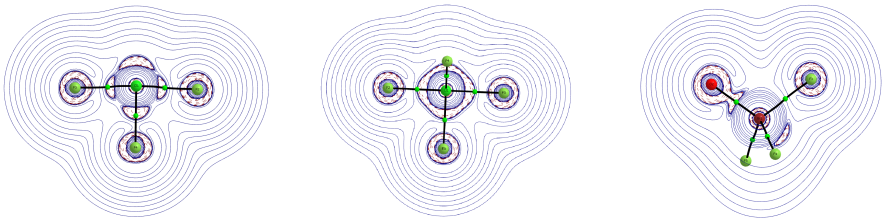

Figure 8: Laplacian of the electron density for chlorine trifluoride, chlorine pentafluoride and bromine trifluoride oxide. All figures in a plane containing the different types of bonds within each molecule. A local charge depletion is seen at the vicinity of the BCPs. Images generated with *AIMall* by analysing *Orca* with the HF method and a def2-TZVP basis set.

It can then be concluded that the charge of the atom, as well as the ionic character of some of the bonds in these molecules provided by QCT, show there is no octet expansion.

5 Conclusions

Chemical information from a wave function can be extracted and interpreted by making use of QCT and QTAIM techniques. The molecular graph can be constructed from the CPs of a molecule, which can be extracted computationally.

Quantum mechanics and the Born-Oppenheimer approximation play a key role regarding molecular geometry. This approximation also simplifies the calculation by expressing the Schrödinger equation solely in electronic terms. The HF method can be used for these type of calculations, providing accurate and reliable results, as well as employing GTO functions, which lower the computational effort.

Methods using electron density, a positive simple function of three coordinates, simplifies the interpretation of the wave function. Extracting information from its Laplacian, which measures local curvature of a function in all its dimensions, provides profitable chemical data and helps reveal further information about the electron density, while supporting the VSEPR theory. The QTAIM emerges from applying QCT to the electron density due to the fact that topology divides the three-dimensional space into atoms, which behave as maxima of the density.

Reliable molecular graphs were constructed for all molecules by making use of QTAIM studies through a HF method with a def2-TZVP basis set, proved by validation in being the most suitable basis set for the development of this thesis, finding a satisfactory compromise between accuracy and computational effort. QCT and QTAIM provides information about CPs, with which molecular graphs can be built. Equivalency between CPs arises to finding point group symmetries and simplifying the amound of data. All molecules studied were expected to be neutral, which was checked using their atomic charges.

It was found that all bonds in the aliphatic hydrocarbons studied had covalent character with different bond strength and multiplicity, as expected. Thanks to the delocalisation index, it is proved that ethane, ethene and ethyne have single, double and triple character in their C-C bonds, respectively. Electron density in RCPs for cyclic compounds decreases when increasing the C-C-C angle, and local charge depletion is shown by positive values of Laplacian. Distinctions between axial and equatorial hydrogens were made for the case of cyclobutane and cyclohexane. Whether a compound is aromatic was checked by examining ellipticity values and delocalisation indexes, which can be used to sense π character. Dipole moments were also extracted with QTAIM and QCT methods, as it was done in the case of polar inorganic compounds: low values of DI in BCPs are due to polarity. If the position of BCPs is added to the molecular graph, structural differences can be found between molecules with the same point group symmetry, as it can be shown for the P-H bonds in phosphine as compared to the N-H bonds in ammonia. In agreement with modern thinking, it was also proved that octet expansion does not happen in the hypervalent halogens studied. Their atomic charges and delocalisation indexes – as well as the positive value of the Laplacian – find ionic character in most bonds forming these molecules, respecting the constrain of having 8 electrons around each atom.

6 References

1. Slater, J. C. The Theory of Complex Spectra. *Phys. Rev.* 1929, *34* (10), 1293–1322.

2. Styer, D. F. *The Strange World of Quantum Mechanics*; Cambridge University Press: Cambridge, England, 2000.

3. Berman, P. R. *Introductory Quantum Mechanics: A Traditional Approach Emphasizing Connections with Classical Physics*, 1st ed.; Springer International Publishing: Basel, Switzerland, 2017.

4. Jensen, F. *Introduction to Computational Chemistry*, 2nd ed.; John Wiley & Sons: Chichester, UK, 2006.

5. Szabo, A.; Ostlund, N. S. *Modern Quantum Chemistry: Introduction to Advanced Electronic Structure Theory*; Dover Publications: Mineola, NY, 1996.

6. Roothaan, C. C. J. New Developments in Molecular Orbital Theory. *Rev. Mod. Phys.* 1951, *23* (2), 69–89.

7. Helgaker, T.; Jørgensen, P.; Olsen, J. *Molecular Electronic-Structure Theory: Helgaker/Molecular Electronic-Structure Theory*; John Wiley & Sons, Ltd: Chichester, UK, 2000.

8. Slater, J. C. Atomic Shielding Constants. *Phys. Rev.* **1930**, *36* (1), 57–64.

9. Boys, S. F. Electronic Wave Functions - I. A General Method of Calculation for the Stationary States of Any Molecular System. *Proc. R. Soc. Lond.* **1950**, *200* (1063), 542–554.

10. Mulliken, R. S. Criteria for the Construction of Good Self-consistent-field Molecular Orbital Wave Functions, and the Significance of LCAO-MO Population Analysis. *J. Chem. Phys.* **1962**, *36* (12), 3428–3439.

11. Löwdin, P.-O. On the Nonorthogonality Problem. In *Advances in Quantum Chemistry Volume 5*; Elsevier, 1970; pp 185–199.

12. Weinstein, H.; Politzer, P.; Srebrenik, S. A Misconception Concerning the Electronic Density Distribution of an Atom. *Theoret. Chim. Acta* **1975**, *38* (2), 159–163.

13. Parr, R. G.; Weitao, Y. *Density-Functional Theory of Atoms and Molecules*; Oxford University Press: London, England, 1994.

14. Gillespie, R. J.; Hargittai, I. *The Vsepr Model of Molecular Geometry*; Dover Publications: Mineola, NY, 2013.

15. Popelier, P. *Atoms in Molecules: An Introduction*; Longman: London, England, 1999.

16. Bader, R. F. W.; Anderson, S. G.; Duke, A. J. Quantum Topology of Molecular Charge Distributions. 1. *J. Am. Chem. Soc.* **1979**, *101* (6), 1389–1395.

17. Keith, T. A.; Gristmill, T. K. *AIMAll Software*; 2019.

18. Neese, F. The ORCA Program System: The ORCA Program System. *Wiley Interdiscip. Rev. Comput. Mol. Sci.* **2012**, *2* (1), 73–78.

19. Bader, R. F. W. *Atoms in Molecules: A Quantum Theory*; Clarendon Press: Oxford, England, 1994.

20. Martín Pendás, Á. *Análisis de la Densidad Electrónica*; Universidad de Oviedo, 2003.

21. Outeiral, C.; Vincent, M. A.; Martín Pendás, Á.; Popelier, P. L. A. Revitalizing the Concept of Bond Order through Delocalization Measures in Real Space. *Chem. Sci.* **2018**, *9* (25), 5517–5529.

22. Hanwell, M. D.; Curtis, D. E.; Lonie, D. C.; Vandermeersch, T.; Zurek, E.; Hutchison, G. R. Avogadro: An Advanced Semantic Chemical Editor, Visualization, and Analysis Platform. *J. Cheminform.* **2012**, *4* (1), 17.

23. Clementi, E.; Popkie, H. Study of the Electronic Structure of Molecules. XVII. Analysis of the Formation of the Acetylene, Ethylene, and Ethane Molecules in the Hartree-Fock Model. *J. Chem. Phys.* **1972**, *57* (11), 4870–4883.

24. Linstrom, P. NIST Chemistry WebBook, NIST Standard Reference Database 69, 1997. https://doi.org/10.18434/T4D303. Date of access: 4th of May 2021.